Laser and Particle Beams (2011), *29*, 345–351.

doi:10.1017/S0263034611000395

Dependence of laser accelerated protons on laser energy following the interaction of defocused, intense laser pulses with ultra-thin targets

C.M. BRENNER,[1,2] J.S. GREEN,[2] A.P.L. ROBINSON,[2] D.C. CARROLL,[1] B. DROMEY,[3] P.S. FOSTER,[2] S. KAR,[3] Y.T. LI,[4] K. MARKEY,[2,3] C. SPINDLOE,[2] M.J.V. STREETER,[2] M. TOLLEY,[2] C.-G. WAHLSTRÖM,[5] M.H. XU,[4] M. ZEPF,[3] P. MCKENNA,[1] AND D. NEELY[2]

[1]Department of Physics, University of Strathclyde, Glasgow, United Kingdom
[2]Central Laser Facility, STFC, Rutherford Appleton Laboratory, Didcot, Oxon, United Kingdom
[3]Centre for Plasma Physics, Queen's University Belfast, Belfast, United Kingdom
[4]Beijing National Laboratory for Condensed Matter Physics, Institute of Physics, Chinese Academy of Sciences, Beijing, China
[5]Department of Physics, Lund University, Lund, Sweden

(RECEIVED 21 March 2011; ACCEPTED 20 June 2011)

Abstract

The scaling of the flux and maximum energy of laser-driven sheath-accelerated protons has been investigated as a function of laser pulse energy in the range of 15–380 mJ at intensities of 10^{16}–10^{18} W/cm^2. The pulse duration and target thickness were fixed at 40 fs and 25 nm, respectively, while the laser focal spot size and drive energy were varied. Our results indicate that while the maximum proton energy is dependent on the laser energy and laser spot diameter, the proton flux is primarily related to the laser pulse energy under the conditions studied here. Our measurements show that increasing the laser energy by an order of magnitude results in a more than 500-fold increase in the observed proton flux. Whereas, an order of magnitude increase in the laser intensity generated by decreasing the laser focal spot size, at constant laser energy, gives rise to less than a tenfold increase in observed proton flux.

Keywords: Flux scaling; Laser plasma acceleration; Laser; Laser-driven ion acceleration; Proton

INTRODUCTION

The acceleration of ions from solid targets irradiated by short (< ps), intense laser pulses is a burgeoning area of research, currently attracting large interest worldwide. The properties of laser-driven ion beams (high brightness and laminarity, ultra-short bunch duration) are, in several respects, markedly different from those of "conventional" accelerator beams. In view of these properties, laser-driven ion beams have the potential to be employed in a number of innovative applications in scientific, technological, and future medical research areas (Borghesi *et al.*, 2005; Malka *et al.*, 2008; Weichsel *et al.*, 2008). However, in order to tailor these laser accelerated ion beams to make them appropriate for applications such as proton heating (Roth *et al.*, 2001; Lefebvre *et al.*, 2009; Pelka *et al.*, 2010), radiography (Cobble *et al.*, 2002) or probing of electric fields (Romagnani *et al.*, 2008), ion beam parameters such as total proton flux need to be both tunable and reproducible. Currently, there are many groups that are concentrating their efforts on discovering an optimum combination of laser and target parameters so as to achieve the desired ion beam properties.

At the laser intensities of interest in this paper (3×10^{16}–10^{18} W/cm^2), it is considered that target normal sheath acceleration (TNS) (Wilks *et al.*, 2001) of ions is the dominant acceleration mechanism. Upon interaction with a pre-formed plasma on the front surface of a target foil, the large electromagnetic fields of the laser pulse act to accelerate electrons up to relativistic energies into the target. A charge separation exists as soon as some of those electrons penetrate through the rear surface of the target foil, leaving behind a strong, electrostatic sheath field (TV/m), which then ionizes and accelerates atoms on the rear surface up to multi-MeV energies over micron scale

Address correspondence and reprint requests to: Ceri M. Brenner, Room 2-60, R1, Central Laser Facility, Rutherford Appleton Laboratory, Didcot, Oxon, OX11 0QX, United Kingdom. E-mail: ceri.brenner@stfc.ac.uk

M.J.V. Streeter is currently at: Blackett Laboratory, Imperial College, London, United Kingdom.

lengths. There are many types of lasers available for experimental research of ion acceleration, however those offering high shot repetition rate are useful for applicative use of this acceleration technique. Currently, laser technology that fulfils this requirement dictates that the laser energy is delivered in the form of very short pulse lengths, circa 40 fs, in order to reach the threshold intensities needed for MeV ion acceleration. Such laser systems are affordable and readily available to many groups for table-top particle acceleration use. It is therefore important to have a good understanding of how the laser driven ion acceleration mechanism responds under these conditions.

In this experiment, we explore proton acceleration using a short pulse, high repetition rate laser operating at, and just below, the relativistic intensity regime (10^{18} W/cm^2) and determine to what extent the proton beam properties (flux as well as the maximum energy) depend on the laser pulse energy and focal spot size. Such control of the proton beam will be essential for any applications. Many studies have been carried out to investigate how ion beam properties scale with laser intensity and laser pulse duration (Clark *et al.*, 2000; Allen *et al.*, 2003; Schreiber *et al.*, 2006; Esirkepov *et al.*, 2006; Fuchs *et al.*, 2006; Robson *et al.*, 2007), however these have been obtained using very different interaction conditions to the ones presented here. Published material that is more relevant to this interaction regime is available in the literature (McKenna *et al.*, 2002; Oishi *et al.*, 2005), yet a dedicated study into the dependence of proton beam properties on laser drive energy has yet to be reported, thus acting as motivation for this present work.

EXPERIMENTAL SETUP

The experiment was conducted using the Ti:Sapphire Astra laser system, which is capable of producing 40 fs laser pulses, delivering up to 650 mJ of energy onto a target when operated in normal contrast mode (2×10^6 at 1 ns before the main pulse), where the contrast is defined as the ratio between the intensity of the main pulse and of the laser prepulse that precedes it. A high contrast ratio was achieved with the use of a single plasma mirror system, which enhanced the contrast to 10^8 at 1 ns before the main pulse. The plasma mirror system (Ziener *et al.*, 2003) consisted of an anti-reflection coated, glass substrate that was positioned in the beam so that it was irradiated with *p*-polarized laser light at an intensity of 5×10^{15} W/cm^2, chosen so as to optimize the reflectivity at the highest laser energy. The plasma mirror efficiency was characterized for each laser energy that was incident on the plasma mirror, peaking at 56% reflectivity. Two $F/8$ off-axis parabolas were used to illuminate the plasma mirror and then recollimate the beam after reflection (see Fig. 1). The plasma mirror was moved after every shot, so that only undamaged areas of the substrate were exposed to the incoming laser pulse. The quality of the reflected beam was confirmed regularly using an equivalent plane monitor that observed a leakage from the last

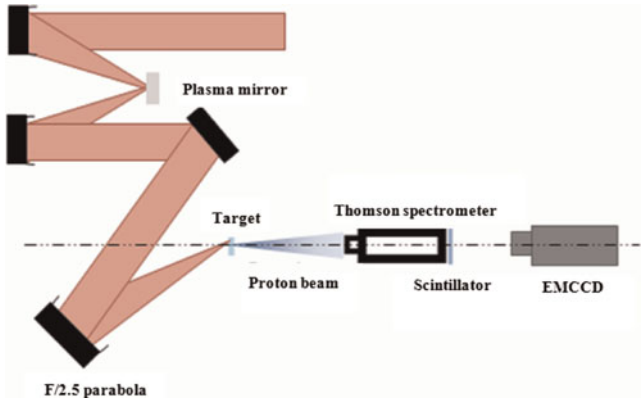

Fig. 1. (Color online) Experimental arrangement with the inclusion of the plasma mirror system.

turning mirror. The beam was then focused onto a 25 nm thick plastic film target at an incident angle of 45°, in *p*-polarized geometry, using an $F/2.5$ off-axis parabola capable of delivering a peak intensity of about 2×10^{19} W/cm^2 with a spot size of 4×6 μm^2 at the best focus position. The optimal distance of the target relative to the focusing parabola for producing the smallest laser spot diameter was achieved to within an accuracy of ± 6 μm and was defined by using a retro-focus system diagnostic (McKenna *et al.*, 2002).

The desired size of the focal spot was measured using an absolutely calibrated equivalent plane monitor and obtained by moving the target toward the focusing parabola along the laser axis. The laser spot intensity distribution away from best focus was measured using a camera lens objective looking directly at the focal spot and was found to have a broadly uniform structure. To avoid pre-plasma formation prior to the leading edge of the main pulse interacting with the front surface of the target, the prepulse intensity was confined to a maximum of about 3×10^{10} W/cm^2, which is well below the plasma formation threshold for a dielectric (Ziener *et al.*, 2003). To achieve this, in addition to the 10^8 contrast provided by the plasma mirror system, a minimum laser spot size of diameter 20 μm was adopted in this campaign, yielding an effective maximum laser intensity of 3.2×10^{18} W/cm^2 at the highest laser energy (380 mJ). The use of an ultrathin target implies that recirculation (Sentoku *et al.*, 2003) within the target will play a significant role during the laser interaction, which has been used to explain enhanced proton signals compared to thicker targets (Mackinnon *et al.*, 2002). We chose to keep the target thickness and laser pulse duration constant, close to optimal values for maximum proton flux determined from earlier studies (Neely *et al.*, 2006) so that scaling could be studied in this region of highest possible flux delivery. In order to study the response of the proton beam flux and maximum energy as a function of laser energy as well as focal spot size, first, the laser energy delivered to the target was varied from about 15 mJ up to about 350 mJ for two focal spot

https://doi.org/10.1017/S0263034611000395 Published online by Cambridge University Press

size diameters of 20 μm and 60 μm and then the laser energy was held constant whilst the focal spot size diameter was varied from 20 μm up to 140 μm.

The diagnostic used for this study was a Thomson parabola ion spectrometer (Carroll *et al.*, 2010) positioned so as to sample the protons accelerated in the target normal direction through a pinhole that subtended a solid angle of 1.1 ± 0.2 μsr. The proton signal was detected using an absolutely calibrated scintillator (Green *et al.*, 2011) that was optically coupled to an Electron Multiplying Charge Couple Device (EMCCD) to give instantaneous spectra over the range 0.15–5 MeV for protons.

RESULTS

The proton spectra obtained for varying laser drive energies are plotted in Figure 2, for a laser spot size of 20 μm and 60 μm. Figure 2a shows that both the proton flux and maximum proton energy increase with increasing laser intensity. Using similar drive laser energies, the scan was repeated but with an approximately nine times larger area of laser irradiation and the resulting spectra plotted in Figure 2b. We note that for the lowest laser energy using a 60 μm spot size (where the laser intensity is 1.9×10^{16} W/cm^2), we are operating very close to the 0.15 MeV proton detection threshold of the spectrometer, yet still producing resolvable data. Comparing the features of Figure 2a to those of Figure 2b, we find that the spectra exhibit broadly similar behavior. The absolute numbers of protons sampled through the pinhole are comparable, if not higher at lower proton energies (<0.75 MeV), for the larger laser spot size despite the intensities on target being an order of magnitude lower. In the paper by Green *et al.* (2010), a similar observation was attributed to the effects of the rear surface source size in combination with the drive intensity. Examining our results in search of underlying trends, the proton flux sampled through the pinhole (integrated over all detected proton energies, E_p, where $0.15 < E_p < 2.5$ MeV) and maximum proton energy, E_{pmax}, were plotted as functions of both laser intensity, I_L, and laser energy, E_L (see Fig. 3). For clarity, changes in the laser intensity brought about by changing the laser energy will be referred to as "varying laser energy" and changes in the laser intensity brought about by changing the laser spot size will be referred to as "varying laser spot size."

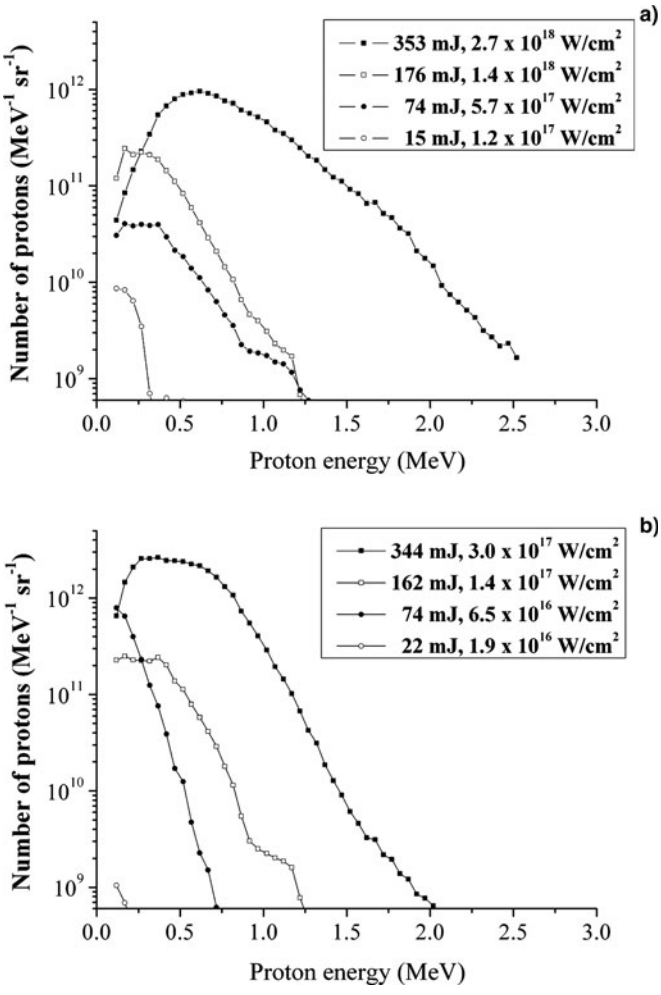

Fig. 2. Experimentally measured proton energy spectra for a laser spot diameter of 20 μm (above) and 60 μm (below).

It is remarkable to note that from Figures 3a–3d, only Figure 3d shows close matching of the two data sets indicating a weak dependence of the proton flux on the laser spot size. The proton flux from both illumination conditions demonstrates an increase of almost 1000 times for an increase in laser energy of only 20 times, with both data sets overlapping in Figure 3d despite there being almost an order of magnitude difference in intensity between the shots taken with the 20 μm and 60 μm focal spot diameter.

In order to further investigate the flux dependence on geometry, additional proton spectra were obtained using maximum laser energy but varying the laser spot size between 20 and 140 μm diameters (see Fig. 4). Again, the proton numbers and maximum energy increase with increasing laser intensity. The integrated proton signal has been plotted as a function of laser intensity (by varying laser spot size) in Figure 5. For constant laser energy, one can see the effect of the laser spot size on the proton signal and how the integrated proton flux is not optimized at the smallest illumination size (20 μm) studied here, which is in good agreement with the results of Green *et al.* (2010). We also observe that even though the intensity has increased by approximately 50 times by varying the laser spot size only, the integrated proton flux has only increased to within an order of magnitude, which is in stark contrast to when the laser energy is varied. Finally, Figure 6 shows the proton flux plotted against laser energy with the inclusion of the integrated proton flux measured at laser spot sizes of 100 μm and 140 μm. A clear scaling relation between the integrated proton flux and laser energy can be fitted with an exponent that goes as $E_L^{2.1 \pm 0.3}$. The consistency of the scaling of the proton flux with laser energy over such a large intensity range

https://doi.org/10.1017/S0263034611000395 Published online by Cambridge University Press

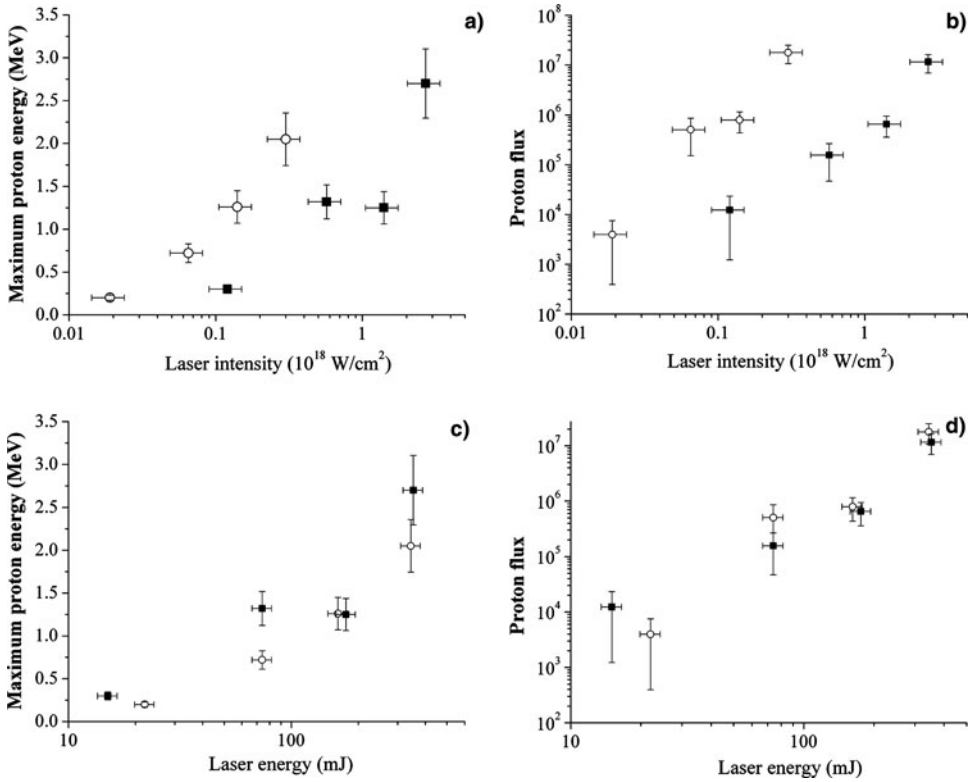

Fig. 3. Investigating the effect of laser illumination geometry on maximum proton energy (**a**, **c**) and integrated proton flux through the pinhole (**b**, **d**), plotted against laser intensity and laser energy, for two laser spot size diameters 20 μm (filled squares) and 60 μm (hollow circles). In the four graphs of the same shots, it is clear that only in figure 3d do both the data sets overlap, indicating that the geometry does not appear to play a significant role.

serves to validate that the proton flux is primarily dependent on the laser energy over the range of conditions studied here.

The maximum proton energy has been plotted as a function of intensity in the case of changing laser energy (Figs. 3a and 3c) and then as a function of intensity in the case of changing focal spot size (Fig. 5). For constant laser energy (see Fig. 5), the maximum proton energy increases slowly, from 0.7 MeV up to 2.7 MeV, over an increase in the intensity of approximately 50 times when the focal spot size is varied. When one compares the trend for changing focal spot size to changing laser energy, we observe a slightly faster scaling relation for varying laser energy. As Figures 3a and 3c shows, plotting E_{pmax} as a function of I_{L} or E_{L} demonstrates a relation (for a given illumination size), whereby a gain in E_{pmax} of almost 10 times is achieved for an increase

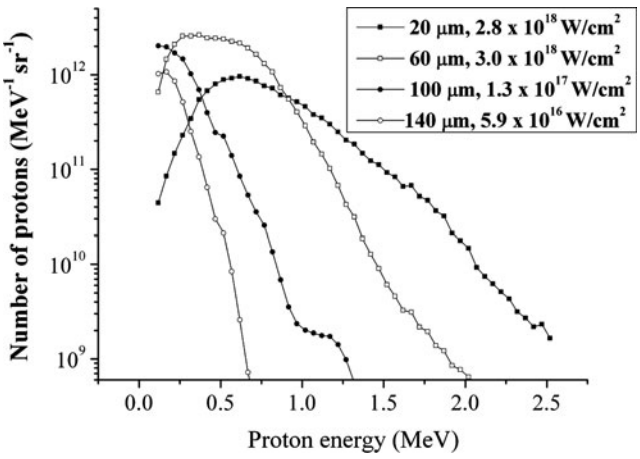

Fig. 4. Experimentally measured proton spectra for constant laser energy (380 ± 40 mJ) at varying laser spot size.

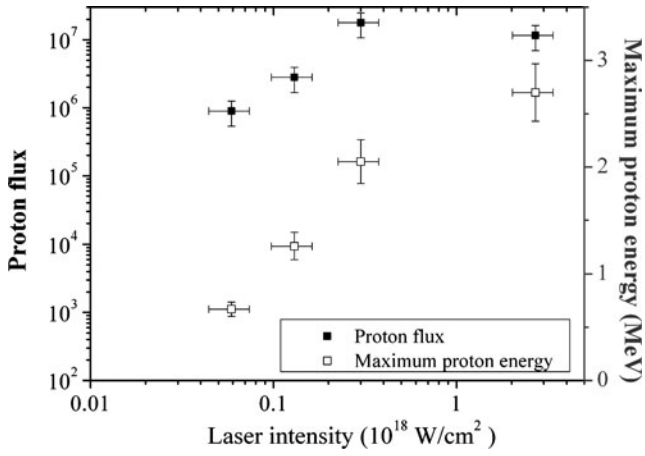

Fig. 5. Maximum proton energy (hollow squares) and integrated proton flux sampled through the pinhole (filled squares) plotted against laser intensity for constant laser energy (380 ± 40 mJ) and varying laser spot size.

https://doi.org/10.1017/S0263034611000395 Published online by Cambridge University Press

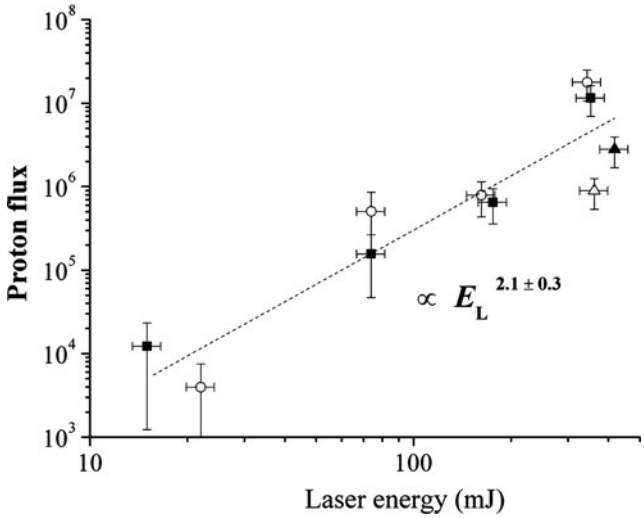

Fig. 6. Integrated proton flux plotted sampled through the pinhole against laser energy for a laser spot size of diameter 20 μm (filled squares), 60 μm (hollow circles), 100 μm (filled triangle) and 140 μm (hollow triangle), highlighting the significant role that laser energy plays in determining the proton flux obtained.

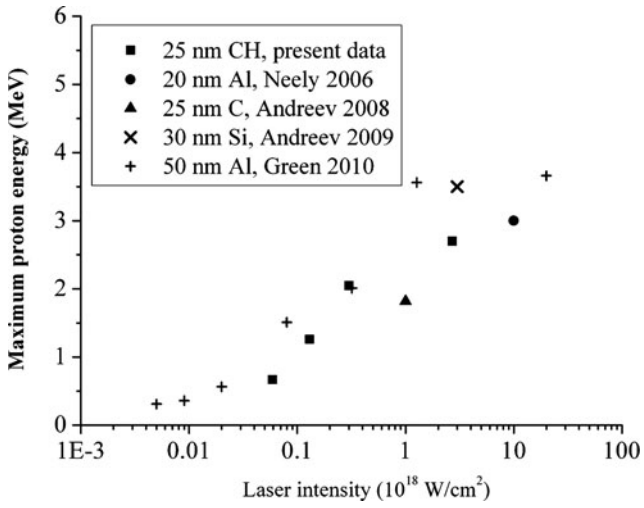

Fig. 7. Maximum proton energy as a function of laser intensity in the regime of high contrast, ultra-short laser pulse interaction with ultra-thin foils measured experimentally here and by Neely *et al.* (2006), Andreev *et al.* (2008, 2009), and Green *et al.* (2010).

in laser energy of approximately 20 times. From Figure 3c, it is also clear that E_{pmax} is a convolution of the two parameters and indeed that, for a given laser energy, the absolute value will be geometry dependent, increasing with smaller spot size.

DISCUSSION

The response of the proton flux of TNS driven systems to a change in laser intensity generated by changing the laser energy has been investigated by other groups using fs laser pulses (Oishi *et al.*, 2005) and longer (Fuchs *et al.*, 2006; Robson *et al.*, 2007). It is worth noting that similar experimental observations to those reported here can be seen in the work published by Oishi *et al.* (2005), whereby scaling relations for maximum proton energy were investigated using short pulses (55 fs to 400 fs) in the intensity range 10^{17}–10^{19} W/cm^2. Their proton spectra show remarkable similarities to the spectra that have been observed above, despite there being a sizeable difference in the laser contrast conditions and target thickness (5 μm). Oishi *et al.* (2005) were able to vary the laser irradiation conditions by changing the laser pulse duration, rather than the focal spot size, yet still they produced an almost identical set of spectra when the laser energy was held constant, and a severe degradation of the proton spectra when the laser energy was reduced from 120 mJ to 43 mJ at a laser pulse duration of 55 fs, in very good agreement with our measurements. This comparison leads one to infer that the driving mechanism behind the correlation of proton flux with E_L could be weakly dependent on plasma scale length on the front surface and electron recirculation. By displaying a very similar pattern of behavior over the two interaction conditions, this serves to highlight the robust and global nature of the strong dependence of the proton flux on the laser energy, for TNS produced proton beams.

Aside from the proton flux dependence, another interesting observation is of the scaling of the maximum proton energy with laser intensity. Assuming that the maximum energy of the proton beam produced can be linearly correlated to the temperature of the relativistic electrons that are directly accelerated by the laser at the front surface (Lefebvre *et al.*, 2010), according to the scaling of Beg *et al.* (1997) the peak proton energies would be expected to scale as $I_L^{0.33}$ for $I_L < 10^{19}$ W/cm^2, which is in close agreement with our trend for varying laser focal spot diameter (see Fig. 5). Furthermore, comparing our measured values of E_{pmax} at maximum laser energy with an accumulation of those that have been achieved with similar laser drive energy and under similar conditions (high contrast, ultra-short pulses interacting with an ultra-thin target), we find that they are also in very good agreement with the slowly varying increase over the intensity range of interest (see Fig. 7), with the trend continuing above the limited intensity of the present work. Figures 3a and 3c further demonstrate that the laser focal spot size is a factor in determining the maximum proton energy; however they also suggest that it is a weaker dependence compared to the scaling of E_{pmax} with laser energy. An observed difference in the scaling of maximum proton energies, depending on whether one changes the laser energy or the focal spot size, has also been reported in parametric investigations of target normal sheath accelerated proton beams (Passoni *et al.*, 2010) wherein ultra-short pulse (25 fs) interactions were investigated in the intensity range 10^{18}–10^{20} W/cm^2.

CONCLUSION

The proton flux data presented here demonstrates a strong dependence on the laser energy ($E_L^{2.1\pm0.3}$) and these findings

https://doi.org/10.1017/S0263034611000395 Published online by Cambridge University Press

are in agreement with the experimental data of others under a wide range of pulse durations and target parameters. The maximum proton energies achieved appear to follow a somewhat slower scaling, in line with what is expected from a TNS driven system and as has been observed by other groups, with the dependence being stronger when changing the laser energy for a fixed laser spot size, as compared to changing the focal spot size for a given laser energy.

This work points towards a method of controlling the proton dose delivered by a laser-driven proton beam through careful control of the laser energy and illumination conditions employed. This observation merits further investigation if we are to succeed in optimizing laser driven ion acceleration for applications.

Our investigation sought to determine the scaling relation between the proton flux and laser energy and how, or if, this relation is affected by laser spot diameter. In doing so, we have highlighted the need to differentiate between changes in laser intensity produced by either a change in laser energy or laser focal spot conditions, as evidently the two should not be combined under simple scaling laws. However it is hoped that based on the studies carried out here and by others, models can be developed with full predictive capability.

ACKNOWLEDGMENTS

The authors would like to acknowledge the expert support of the laser, engineering and target fabrication staff of the Central Laser Facility. This work was supported as part of the LIBRA EPSRC grant EP/E035728/1.

REFERENCES

Allen, M., Sentoku, Y., Audebert, P., Blazevic, A., Cowan, T., Fuchs, J., Gauthier, J.C., Geissel, M., Hegelich, M., Karsch, S., Morse, E., Patel, P.K. & Roth, M. (2003). Proton spectra from ultraintense laser-plasma interaction with thin foils: Experiments, theory, and simulation. *Phys. Plasmas* **10**, 3283–3289.

Andreev, A., Levy, A., Ceccotti, T., Thaury, C., Platonov, K., Loch, R.A. & Martin, P. (2008). Fast-Ion energy-flux enhancement from ultrathin foils irradiated by intense and high-contrast short laser pulses. *Phys. Rev. Lett.* **101**, 155002/1–4.

Andreev, A.A., Steinke, S., Sokollik, T., Schnurer, M., Ter, Avetsiyan, S., Platonov, K.Y. & Nickles, P.V. (2009). Optimal ion acceleration from ultrathin foils irradiated by a profiled laser pulse of relativistic intensity. *Phys. Plasmas* **16**, 1–9.

Beg, F.N., Bell, A.R., Dangor, A.E., Danson, C.N., Fews, A.P., Glinsky, M.E., Hammel, B.A., Lee, P., Norreys, P.A. & Tatarakis, M. (1997). A study of picosecond laser-solid interactions up to 10^{19} Wcm^{-2}. *Phys. Plasmas* **4**, 447–457.

Borghesi, M., Audebert, P., Bulanov, S.V., Cowan, T., Fuchs, J., Gauthier, J.C., Mackinnon, A.J., Patel, P.K., Pretzler, G., Romagnani, L., Schiavi, A., Toncian, T. & Willi, O. (2005). High-intensity laser-plasma interaction studies employing laser-driven proton probes. *Laser Part. Beams* **23**, 291–295.

Carroll, D.C., Brummitt, P., Neely, D., Lindau, F., Lundh, O., Wahlstrom, C.G. & Mckenna, P. (2010). A modified Thomson parabola spectrometer for high resolution multi-MeV ion measurements-Application to laser-driven ion acceleration. *Nucl. Instr. Meth. Phys. Res. Sect. A* **620**, 23–27.

Clark, E.L., Krushelnick, K., Zepf, M., Beg, F.N., Tatarakis, M., Machacek, A., Santala, M.I.K., Watts, I., Norreys, P.A. & Dangor, A.E. (2000). Energetic heavy-ion and proton generation from ultraintense laser-plasma interactions with solids. *Phys. Rev. Lett.* **85**, 1654–1657.

Cobble, J.A., Johnson, R.P., Cowan, T.E., Renard-Le Galloudec, N. & Allen, M. (2002). High resolution laser-driven proton radiography. *J. Appl. Phys.* **92**, 1775–1779.

Esirkepov, T., Yamagiwa, M. & Tajima, T. (2006). Laser ion-acceleration scaling laws seen in multiparametric particle-in-cell simulations. *Phys. Rev. Lett.* **96**, 105001/1–4.

Fuchs, J., Antici, P., D'humieres, E., Lefebvre, E., Borghesi, M., Brambrink, E., Cecchetti, C.A., Kaluza, M., Malka, V., Manclossi, M., Meyroneinc, S., Mora, P., Schreiber, J., Toncian, T., Pepin, H. & Audebert, R. (2006). Laser-driven proton scaling laws and new paths towards energy increase. *Nat. Phys.* **2**, 48–54.

Green, J.S., Borghesi, M., Brenner, C.M., Carroll, D.C., Dover, N.P., Foster, P.S., Gallegos, P., Green, S., Kirby, D., Kirkby, K.J., Mckenna, P., Merchant, M.J., Najmudin, Z., Palmer, C.A.J., Parker, D., Prasad, R., Quinn, K.E., Rajeev, P.P., Read, M.P., Romagnani, L., Schreiber, J., Streeter, M.J.V., Tresca, O., Zepf, M. & Neely, D. (2011). Scintillator-based ion beam profiler for diagnosing laser-accelerated ion beams. *SPIE*. http://spiedigitallibrary.org/proceedings/resource/2/psisdg/8079/1/807919_1?isAuthorized=no.

Green, J.S., Carroll, D.C., Brenner, C., Dromey, B., Foster, P.S., Kar, S., Li, Y.T., Markey, K., Mckenna, P., Neely, D., Robinson, A.P.L., Streeter, M.J.V., Tolley, M., Wahlstrom, C.G., Xu, M.H. & Zepf, M. (2010). Enhanced proton flux in the MeV range by defocused laser irradiation. *New J. Phys.* **12**, 085012/1–10.

Lefebvre, E., Carrie, M. & Nuter, R. (2009). Ion acceleration with high-intensity lasers and application to isochoric heating. *Comp. Rendus Phys.* **10**, 197–206.

Lefebvre, E., Gremillet, L., Levy, A., Nuter, R., Antici, P., Carrie, M., Ceccotti, T., Drouin, M., Fuchs, J., Malka, V. & Neely, D. (2010). Proton acceleration by moderately relativistic laser pulses interacting with solid density targets. *New J. Phys.* **12**, 045017/1–15.

Mackinnon, A.J., Sentoku, Y., Patel, P.K., Price, D.W., Hatchett, S., Key, M.H., Andersen, C., Snavely, R. & Freeman, R.R. (2002). Enhancement of proton acceleration by hot-electron recirculation in thin foils irradiated by ultraintense laser pulses. *Phys. Rev. Lett.* **88**, 215006/1–4

Malka, V., Faure, J., Gauduel, Y.A., Lefebvre, E., Rousse, A. & Phuoc, K.T. (2008). Principles and applications of compact laser-plasma accelerators. *Nat. Phys.* **4**, 447–453.

Mckenna, P., Ledingham, K.W.D., Spencer, I., Mccany, T., Singhal, R.P., Ziener, C., Foster, P.S., Divall, E.J., Hooker, C.J., Neely, D., Langley, A.J., Clarke, R.J., Norreys, P.A., Krushelnick, K. & Clark, E.L. (2002). Characterization of multiterawatt laser-solid interactions for proton acceleration. *Rev. Sci. Instr.* **73**, 4176–4184.

Neely, D., Foster, P., Robinson, A., Lindau, F., Lundh, O., Persson, A., Wahlstrom, C.G. & Mckenna, P. (2006). Enhanced proton beams from ultrathin targets driven by high contrast laser pulses. *Appl. Phys. Lett.* **89**, 021502/1–3.

Oishi, Y., Nayuki, T., Fujii, T., Takizawa, Y., Wang, X., Yamazaki, T., Nemoto, K., Kayoiji, T., Sekiya, T., Horioka, K., Okano, Y., Hironaka, Y., Nakamura, K.G., Kondo, K. & Andreev, A.A. (2005). Dependence on laser intensity and pulse duration in proton acceleration by irradiation of ultrashort laser pulses on a Cu foil target. *Phys. Plasmas* **12**, 073102/1–5.

Passoni, M., Bertagna, L. & Zani, A. (2010). Target normal sheath acceleration: theory, comparison with experiments and future perspectives. *New J. Phys*. **12**, 045012/1–14.

Pelka, A., Gregori, G., Gericke, D.O., Vorberger, J., Glenzer, S.H., Gunther, M.M., Harres, K., Heathcote, R., Kritcher, A.L., Kugland, N.L., Li, B., Makita, M., Mithen, J., Neely, D., Niemann, C., Otten, A., Riley, D., Schaumann, G., Schollmeier, M., Tauschwitz, An. & Roth, M. (2010). Ultrafast melting of carbon induced by intense proton beams. *Phys. Rev. Lett*. **105**, 265701/1–4.

Robson, L., Simpson, P.T., Clarke, R.J., Ledingham, K.W.D., Lindau, F., Lundh, O., Mccanny, T., Mora, P., Neely, D., Wahlstrom, C.G., Zepf, M. & Mckenna, P. (2007). Scaling of proton acceleration driven by petawatt-laser-plasma interactions. *Nat. Phys*. **3**, 58–62.

Romagnani, L., Borghesi, M., Cecchetti, C.A., Kar, S., Antici, P., Audebert, P., Bandhoupadjay, S., Ceccherini, F., Cowan, T., Fuchs, J., Galimberti, M., Gizzi, L.A., Grismayer, T., Heathcote, R., Jung, R., Liseykina, T.V., Macchi, A., Mora, P., Neely, D., Notley, M., Osterholtz, J., Pipahl, C.A., Pretzler, G., Schiavi, A., Schurtz, G., Toncian, T., Wilson, P.A. & Willi, O. (2008). Proton probing measurement of electric and magnetic fields generated by ns and ps laser-matter interactions. *Laser Part. Beams* **26**, 241–248.

Roth, M., Cowan, T.E., Key, M.H., Hatchett, S.P., Brown, C., Fountain, W., Johnson, J., Pennington, D.M., Snavely, R.A., Wilks, S.C., Yasuike, K., Ruhl, H., Pegoraro, F., Bulanov, S.V., Campbell, E.M., Perry, M.D. & Powell, H. (2001). Fast ignition by intense laser-accelerated proton beams. *Phys. Rev. Lett*. **86**, 436–439.

Schreiber, J., Bell, F., Gruner, F., Schramm, U., Geissler, M., Schnurer, M., Ter-Avetisyan, S., Hegelich, B.M., Cobble, J., Brambrink, E., Fuchs, J., Audebert, P. & Habs, D. (2006). Analytical model for ion acceleration by high-intensity laser pulses. *Phys. Rev. Lett*. **97**, 045005/1–4.

Sentoku, Y., Cowan, T.E., Kemp, A. & Ruhl, H. (2003). High energy proton acceleration in interaction of short laser pulse with dense plasma target. *Phys. Plasmas* **10**, 2009–2015.

Weichsel, J., Fuchs, T., Lefebvre, E., D'humieres, E. & Oelfke, U. (2008). Spectral features of laser-accelerated protons for radiotherapy applications. *Phys. Med. Biol*. **53**, 4383–4397.

Wilks, S.C., Langdon, A.B., Cowan, T.E., Roth, M., Singh, M., Hatchett, S., Key, M.H., Pennington, D., Mackinnon, A. & Snavely, R.A. (2001). Energetic proton generation in ultra-intense laser-solid interactions. *Phys. Plasmas* **8**, 542–549.

Ziener, C., Foster, P.S., Divall, E.J., Hooker, C.J., Hutchinson, M.H.R., Langley, A.J. & Neely, D. (2003). Specular reflectivity of plasma mirrors as a function of intensity, pulse duration, and angle of incidence. *J. Appl. Physics* **93**, 768–770.

https://doi.org/10.1017/S0263034611000395 Published online by Cambridge University Press